Supporting Information

Unraveling the effects of asymmetric interfaces in three-dimensional solid oxide fuel cells

Young Gyun Goh,[a] *Jeong Hun Kim,*[b,*] *Hyoungchul Kim,*[c,*] *Sung Soo Shin,*[d,*]

[a]School of Mechanical System Engineering, Kumoh National Institute of Technology, 61 Daehak-ro, Gumi, Gyeongbuk 39177, Republic of Korea

[b]Smart Materials Research Section, Electronics and Telecommunications Research Institute, 218 Gajeong-ro, Yuseong-gu, Daejeon, Republic of Korea

[c]Department of Mechanical and System Design Engineering, Hongik University, 94 Wausan-ro, Mapo-gu, Seoul 04066, Republic of Korea

[d]Department of Mechanical Engineering, Incheon National University, 119 Academy-ro, Yeonsu-gu, Incheon 22012, Republic of Korea

AUTHOR INFORMATION

Corresponding Authors

*E-mail: JeongHun@etri.re.kr (J. H. Kim), hyoungchul@hongik.ac.kr (H. Kim), ssshin@inu.ac.kr (S. S. Shin).

Materials and Methods

Fabrication of anode substrate

To fabricate the anode substrate, NiO (Sumitomo) and 8 mol% Y_2O_3-ZrO_2 (yttria-stabilized zirconia, YSZ; Tosoh) powders were combined with KD-1 (Sigma-Aldrich), which served as a dispersant, and polymethylmethacrylate (PMMA; Sunjin Chemical), which served as a pore former, in a solvent mixture consisting of ethyl alcohol and toluene, followed by ball milling with 5- and 10-mm-diameter zirconia balls. Then, dibutyl phthalate and polyvinyl butyral (PVB) were added as a plasticizer and binder, respectively, to enhance the viscosity and ductility of the slurry. Subsequently, the homogeneously dispersed slurry was cast using a tape-casting machine to produce anode supporting layer (ASL) sheets. The anode functional layer (AFL) sheets were fabricated by applying the same process as that for the ASL sheets, with the exception of the absence of PMMA powder. The resulting ASL and AFL sheets were laminated by applying a heat press machine at 5 MPa and 60 °C to fabricate an anode substrate with a thickness of 0.8 mm.

Cell fabrication

A 10-μm prism-structure polyurethane acrylate (PUA) mold was used to implement ceramic micropatterning to achieve a three-dimensional (3D) interface between the anode substrate and electrolyte layer. The PUA mold was fabricated by applying a soft lithography process using a wet-etched Si master mold. After dripping PUA precursor solution onto the Si master mold, covering it with a polyethylene terephthalate film, and subsequently exposing it to ultraviolet light to cure the PUA, the PUA mold was

manufactured. To achieve the 3D ceramic micropatterning of the anode interface, the prepared anode substrate was positioned beneath the PUA mold and subjected to an additional lamination process at 25 MPa and 60 °C. Subsequently, the YSZ electrolyte layer was deposited on the anode substrate via an electrospray deposition process and co-sintered at 1350 °C for 3 h. Pulsed laser deposition and electrospray deposition (ESD) were respectively applied to sequentially coat the sintered substrate with a $Ce_{0.9}Gd_{0.1}O_{2-\delta}$ (CGO; Solvay) buffer layer and $La_{0.6}Sr_{0.4}CoO_{3-\delta}$ (LSC; KCeraCell) cathode layer. The cathode layer was then annealed at 950 °C for 1 h. The active electrode area of all cells was 1 cm^2.

ESD process

During the ESD process, ethyl alcohol was used as the solvent. For the electrolyte deposition, we applied a mixture of 2 wt% YSZ powder and 2 wt% PVB binder (relative to the solvent). The ESD of the electrolyte solution was performed under the following conditions: deposition temperature, room temperature; applied voltage, 7.0 kV; nozzle tip-to-substrate distance, 5 cm; and flow rate, 0.2 ml h^{-1}. For the cathode deposition process, 10 wt% LSC powder was mixed with 10 wt% polyvinylpyrrolidone binder (relative to the solvent). The ESD of the cathode solution was performed under the following conditions: deposition temperature, 110 °C; applied voltage, 6.4 kV; nozzle tip-to-substrate distance, 4 cm; and flow rate, 0.2 ml h^{-1}.

Cell characterization

To measure the electrochemical performance of the fabricated cells, hydrogen gas containing 3% H_2O was fed to the anode, and air was supplied to the cathode at a flow rate of 200 mL min^{-1}. The cell's current density−voltage−power density curves and electrochemical impedance results were obtained by applying an electrochemical analyzer (IviumStat; Ivium Technologies) within the temperature range of 500−650 °C at intervals of 50 °C. Distribution of relaxation times (DRT) analysis was conducted to quantify each resistance component based on the electrochemical impedance results corresponding to the frequency range of 1×10^6 to 1×10^{-1} Hz. We employed FTIKREG software for the DRT analysis to convert data from the time domain to the frequency domain; in this analysis, we applied the optimized regularization parameters based on the L-curve for the minimal solution norm and misfit norm.[1–3] Additionally, we employed a Gaussian distribution model for discretization to enable quantification of the low-frequency resistance (R_{LF}, below 10 Hz), mid-frequency resistance (R_{MF}, 10 Hz to 1 kHz), and high-frequency resistance (R_{HF}, above 1 kHz) from the DRT curves. To quantify the resistance components, the area ratios of each peak within the DRT results were multiplied by the total area-specific polarization resistance (ASR_{pol}). The microstructure of the cell was analyzed using scanning electron microscopy (SEM; MAIA 3 LM; TESCAN).

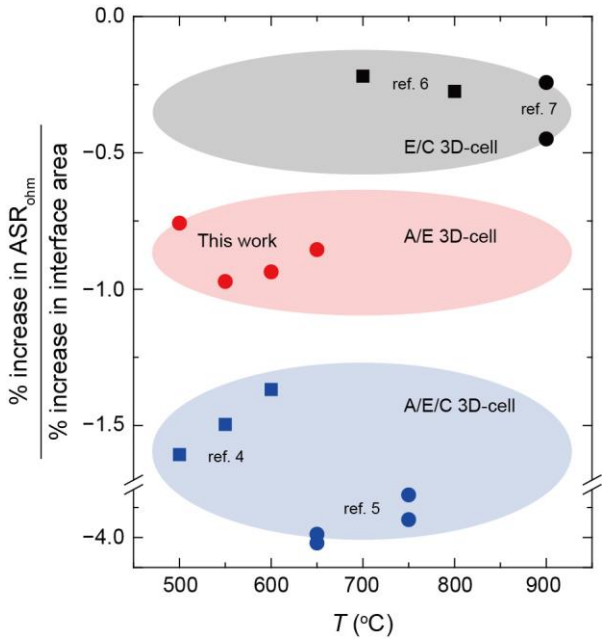

Fig. S1. Comparison of the ASR_{ohm} increase rate divided by interface area increase rate in this work with that of the previously reported A/E/C 3D-cells and E/C 3D-cells.[4-7]

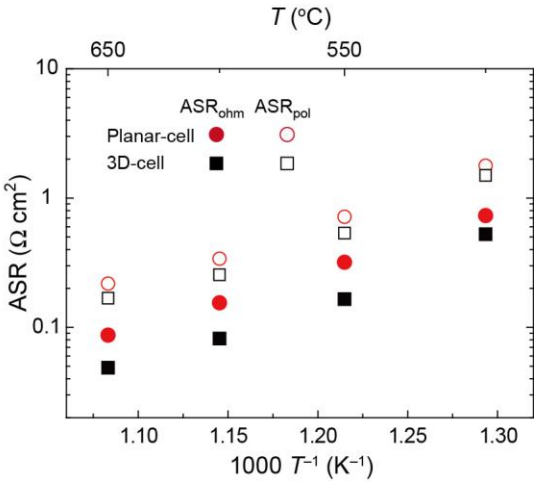

Fig. S2. Arrhenius plot of the ASR_{ohm} and ASR_{pol} for the Planar-cell and 3D-cell under the voltage of 0.75 V and different operating temperatures.

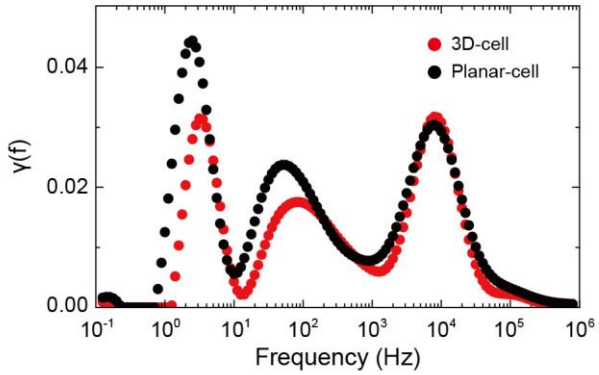

Fig. S3. DRT curves derived from the electrochemical impedance spectra for the Planar-cell and 3D-cell under the voltage of 0.75 V and 650 °C.

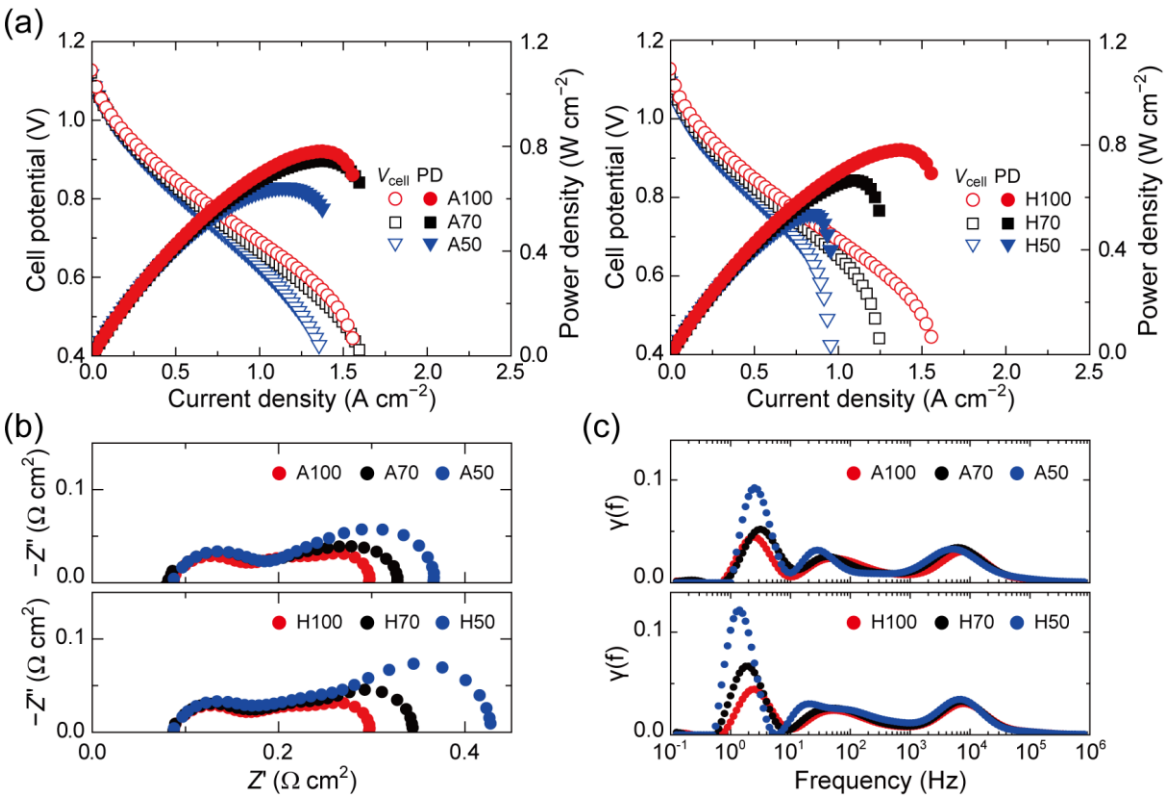

Fig. S4. (a) Current density–voltage–power density curves for the Planar-cell under various partial pressure conditions at 650 °C. (b) Nyquist plots and (c) DRT curves derived from the electrochemical impedance spectra for Planar-cell under various partial pressure conditions at 0.75 V and 650 °C.

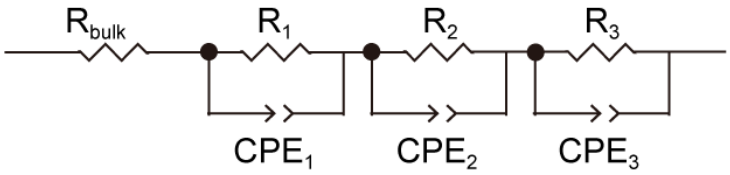

Fig. S5. Used equivalent circuit for the complex non-linear least squares fitting.

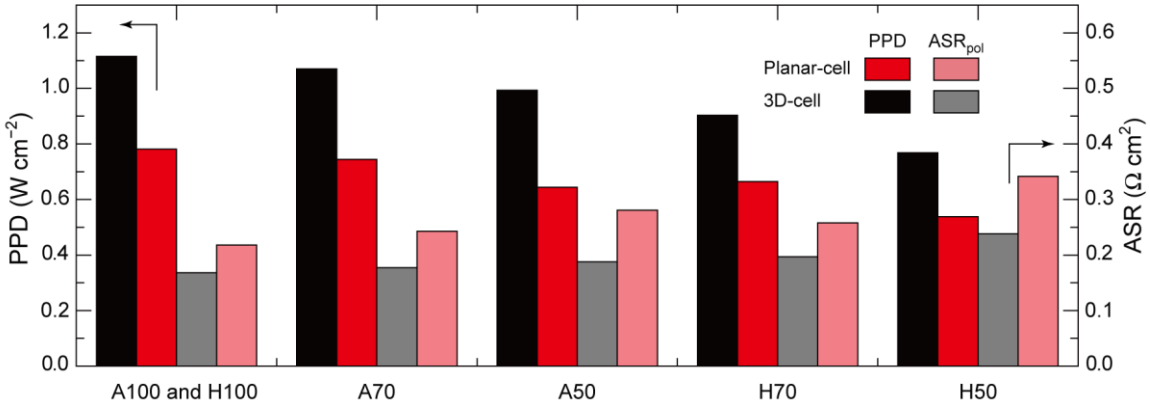

Fig. S6. Graph of quantitative values for PPD and ASR_{pol} for all cells under various gas partial pressure conditions at 0.75 V and 650 °C.

Planar-cell					
	A100&H100	A70	A50	H70	H50
R_{bulk} [Ω cm^2]	0.086	0.084	0.086	0.086	0.086
R_1 [Ω cm^2]	0.078	0.097	0.120	0.081	0.079
CPE-T_1 ($Fs^{\alpha-1}$)	3.331×10^{-3}	4.214×10^{-3}	6.000×10^{-3}	3.044×10^{-3}	2.962×10^{-3}
CPE-P_1 (α)	0.763	0.737	0.712	0.773	0.782
R_2 [Ω cm^2]	0.079	0.079	0.089	0.090	0.139
CPE-T_2 ($Fs^{\alpha-1}$)	0.214	0.283	0.338	0.196	0.308
CPE-P_2 (α)	0.686	0.684	0.708	0.681	0.568
R_3 [Ω cm^2]	0.056	0.069	0.091	0.089	0.126
CPE-T_3 ($Fs^{\alpha-1}$)	1.391	0.950	0.714	1.129	0.946
CPE-P_3 (α)	0.939	0.923	0.991	0.933	0.983
Chi-squared	1.933×10^{-5}	2.230×10^{-5}	1.919×10^{-5}	2.448×10^{-5}	1.775×10^{-5}

3D-cell					
	A100&H100	A70	A50	H70	H50
R_{bulk} [Ω cm^2]	0.053	0.053	0.054	0.054	0.054
R_1 [Ω cm^2]	0.066	0.069	0.076	0.062	0.063
CPE-T_1 ($Fs^{\alpha-1}$)	2.046×10^{-3}	1.903×10^{-3}	2.407×10^{-3}	1.466×10^{-3}	1.518×10^{-3}
CPE-P_1 (α)	0.820	0.825	0.798	0.859	0.857
R_2 [Ω cm^2]	0.062	0.059	0.060	0.079	0.108
CPE-T_2 ($Fs^{\alpha-1}$)	0.210	0.281	0.308	0.256	0.321
CPE-P_2 (α)	0.676	0.656	0.667	0.615	0.550
R_3 [Ω cm^2]	0.033	0.049	0.054	0.050	0.069
CPE-T_3 ($Fs^{\alpha-1}$)	1.559	1.106	0.805	1.307	1.119
CPE-P_3 (α)	0.978	0.871	0.932	0.978	0.997
Chi-squared	2.243×10^{-5}	2.699×10^{-5}	2.780×10^{-5}	3.178×10^{-5}	2.898×10^{-5}

Table S1. Detailed complex non-linear least squares fitting parameters for Planar-cell and 3D-cell under various partial pressure conditions at 0.75 V and 650 °C.

Planar-cell					
	A100&H100	A70	A50	H70	H50
Regularization parameter	0.0083				

3D-cell					
	A100&H100	A70	A50	H70	H50
Regularization parameter	0.0083				

Table S2. The regularization parameters used in DRT analysis for the Planar-cell and 3D-cell.

Planar-cell					
	A100&H100	A70	A50	H70	H50
PPD [W cm^{-2}]	0.781	0.744	0.644	0.656	0.538
ASR_{pol} [Ω cm^2]	0.213	0.245	0.282	0.260	0.345

3D-cell					
	A100&H100	A70	A50	H70	H50
PPD [W cm^{-2}]	1.115	1.070	0.993	0.903	0.768
ASR_{pol} [Ω cm^2]	0.162	0.177	0.190	0.192	0.240

Table S3. PPD and ASR_{pol} for the Planar-cell and 3D-cell under various partial pressure conditions at 650 °C. ASR_{pol} was measured at 0.75 V.

Planar-cell					
	A100&H100	A70	A50	H70	H50
R_{LF} [Ω cm^2]	0.066	0.083	0.122	0.101	0.158
R_{MF} [Ω cm^2]	0.077	0.076	0.076	0.085	0.105
R_{HF} [Ω cm^2]	0.070	0.085	0.084	0.074	0.081

3D-cell					
	A100&H100	A70	A50	H70	H50
R_{LF} [Ω cm^2]	0.042	0.052	0.062	0.064	0.091
R_{MF} [Ω cm^2]	0.057	0.057	0.056	0.067	0.079
R_{HF} [Ω cm^2]	0.063	0.068	0.074	0.061	0.070

Table S4. R_{LF}, R_{MF}, R_{HF} values derived from the DRT curves for the Planar-cell and 3D-cell under various partial pressure conditions at 0.75 V and 650 °C.

References

1 J. Weese, *Comput. Phys. Commun.*, 1992, **69**, 99–111.

2 M.-B. Choi, J. Shin, H.-I. Ji, H. Kim, J.-W. Son, J.-H. Lee, B.-K. Kim, H.-W. Lee and K. J. Yoon, *JOM*, 2019, **71**, 3825–3834.

3 S. S. Shin, J.-S. Kim, S. Choi, H.-I. Ji, K. J. Yoon, J.-H. Lee, K. Y. Chung and H. Kim, *Chem. Commun.*, 2021, **57**, 3453–3456.

4 S. S. Shin, J. H. Kim, K. T. Bae, K.-T. Lee, S. M. Kim, J.-W. Son, M. Choi and H. Kim, *Energy Environ. Sci.*, 2020, **13**, 3459–3468.

5 H. Seo, H. Iwai, M. Kishimoto, C. Ding, M. Saito and H. Yoshida, *J. Power Sources*, 2020, **450**, 227682.

6 C. Lee, S. S. Shin, J. Choi, J. Kim, J.-W. Son, M. Choi and H. H. Shin, *J. Mater. Chem. A*, 2020, **8**, 16534–16541.

7 J. A. Cebollero, R. Lahoz, M. A. Laguna-Bercero and A. Larrea, *J. Power Sources*, 2017, **360**, 336–344.